Available online at www.sciencedirect.com
SCIENCE DIRECT®
International Journal of Heat and Mass Transfer 47 (2004) 4257–4263
International Journal of HEAT and MASS TRANSFER
www.elsevier.com/locate/ijhmt

Disc cooled with high-conductivity inserts that extend inward from the perimeter

A.K. da Silva [a,*], C. Vasile [b], A. Bejan [a]

[a] Department of Mechanical Engineering and Materials Science, Box 90300, Duke University, Durham, NC 27708-0300, USA
[b] Département Génie Climatique et Energétique, Institut National des Sciences, Appliquées de Strasbourg, 24 Boulevard de la Victoire, 67084 Strasbourg, France

Received 15 March 2004; received in revised form 30 April 2004
Available online 2 July 2004

Abstract

This paper considers the fundamental problem of how to shape rectangular high-conductivity inserts (fins) that are mounted on the rim of and protrude into a disc-shaped body that generates heat. The objective is to minimize the global thermal resistance by optimizing geometrically the distribution of a fixed amount of high-conductivity material through the material of lower conductivity. In addition to the fin geometry, three other design parameters are considered: the ratio between the high conductivity and low conductivity $\tilde{k}$, the relative amount of high conductivity material ϕ, and the number of sectors of the disc-shaped body, N. It is shown analytically and numerically that the thermal resistance can be minimized with respect to the fin aspect ratio, λ. The optimized geometry and performance are reported graphically as functions of $\tilde{k}$, ϕ and N. Good agreement is found between the analytical solution and the numerical results.
© 2004 Elsevier Ltd. All rights reserved.

Keywords: Constructal theory; Fins; Heat transfer density; Conduction; Packing; Electronics cooling

1. Introduction

Constructal theory and design [1–3] serves as a reminder that flow systems that must be designed (configured) must be treated as malleable, i.e., as morphing structures that are as free to change as possible. Configurations that are postulated (assumed) based on past practice, handbooks and rules of thumb, are not necessarily the best. The only rule of thumb worth remembering is that geometry must not be taken for granted. Geometry matters, in fact, geometry is a result, not an assumption. It is geometry that endows the flow system with the ability to serve its purpose, in spite of the constraints.

The field of heat transfer has demonstrated for many years how the principle of generating flow geometry works. First and foremost, this principle is one about objective: the need to make things compact, to use the available space to the maximum. The oldest and best documented subfield of heat transfer where the generation of geometry is documented is the geometric optimization of fins [4–11]. This activity is reviewed in a recent treatise [12].

In this paper we address a practical problem, which occurs in several domains, for example, in the cooling of electronic packages and the enhancement of heat transfer in packed bed heat exchangers. The problem is how to cool *from the outside* a space in which heat is generated volumetrically. The generation of heat can be due to Joule heating, as in the case of packages of electronics, or it can be due to convection, as in the flow of a hot gas through a packed bed.

Two recent studies [13,14] have shown how to facilitate the removal of the generated heat when the heat

* Corresponding author. Tel.: +1-919-660-5299; fax: +1-919-660-8963.
E-mail address: akd3@duke.edu (A.K. da Silva).

0017-9310/$ - see front matter © 2004 Elsevier Ltd. All rights reserved.
doi:10.1016/j.ijheatmasstransfer.2004.04.024

Nomenclature

D	fin width, m
k_0	disc thermal conductivity, $\mathrm{W\,m^{-1}\,K^{-1}}$
k_p	fin thermal conductivity, $\mathrm{W\,m^{-1}\,K^{-1}}$
L	fin length, m
N	number of sectors
q'	total heat transfer current, $\mathrm{W\,m^{-1}}$
q''	heat flux, $\mathrm{W\,m^{-2}}$
q'''	heat generation, $\mathrm{W\,m^{-3}}$
R	disc radius, m
R_{th}	global thermal resistance, $\mathrm{m\,KW^{-1}}$
t	disc thickness, m
T	temperature, K
T_{c}	disc center temperature, K
T_h	rim temperature, K
$T_{\max}$	hot spot temperature, K
$T_{\min}$	fin root temperature, K
x, y	Cartesian coordinates, m
$\tilde{y}$	dimensionless fin length

Greek symbols

α	angle, rad
ε	error criterion
λ	fin aspect ratio
ξ	length variable, m
ϕ	fin fraction area

Subscripts

max	maximum
min	minimum

Superscript

$(\sim)$	dimensionless variables

sink is located in the center of a disc-shaped volume. In such cases, it is advantageous to install high-conductivity inserts that extend radially away from the disc center, and bifurcate before they reach the perimeter. Tree-shaped inserts and fins have been optimized in this fashion, and their architecture promises to be more attractive and more complex as the heat generating volumes become larger.

In the present paper we consider the related problem where cooling is available on the outside of the heat generating disc. Instead of high-conductivity trees growing away from the center, we explore the idea of installing high-conductivity inserts that extend inward from the disc perimeter. We optimize the geometry of such populations of inserts analytically and numerically.

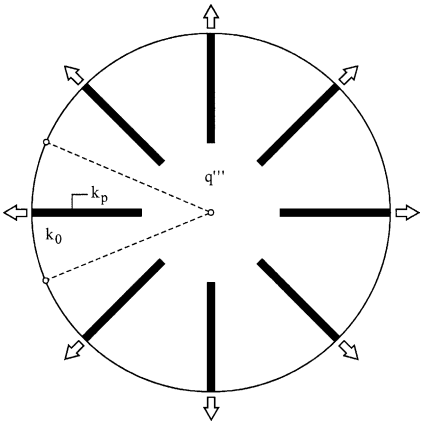

Fig. 1. Disc with uniform heat generation and high-conductivity blades extending inward from the rim.

2. Analytical formulation

A disc of fixed radius R and thermal conductivity k_0 generates heat at the rate q'' per unit area. The generated heat current ($q = q''\pi R^2$) is removed through N radial fins of much higher conductivity (k_p). As shown in Fig. 1, the fins are positioned equidistantly on the disc perimeter, and extend inward. Each fin has the length L and thickness D. The amount of k_p material is fixed. This constraint can be expressed in terms of the fixed area fraction occupied by k_p material on the disc,

$$\phi = \frac{DLN}{\pi R^2} \tag{1}$$

The geometry of the distribution of fin material is represented fully by the elemental sector isolated in Fig. 2. The sector contains one k_p fin and the k_0 material allocated to that fin. The configuration has two degrees of freedom, the fin aspect ratio

$$\lambda = \frac{L}{D} \tag{2}$$

and the angle

$$\alpha = \frac{2\pi}{N} \tag{3}$$

The following analysis is valid in the limit

$$\alpha \ll 1 \quad \phi \ll 1 \quad k_0 \ll k_p \tag{4}$$

in which the sector is approximated by an isosceles triangle (Fig. 2). In this limit, conduction through the fin is oriented radially, and conduction through the material adjacent to the fin is oriented azimuthally.

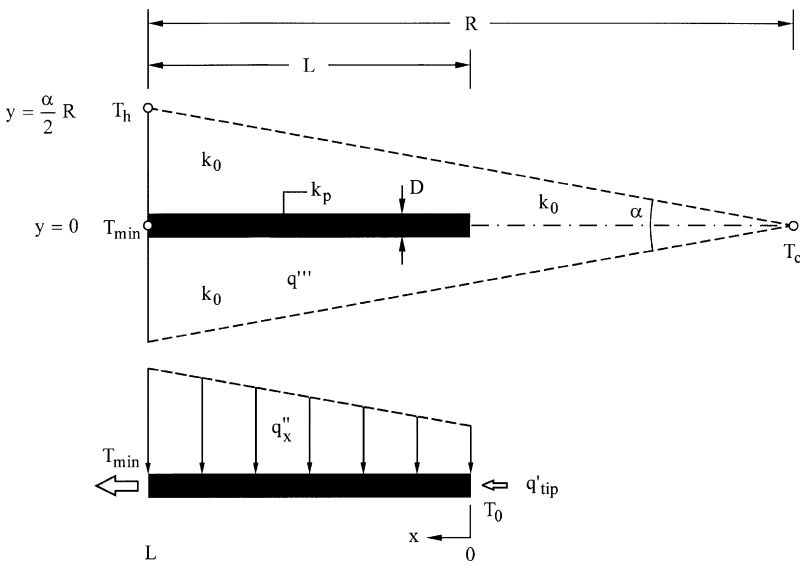

Fig. 2. Triangular model of one of the N sectors of the disc cross-section.

The objective is to find the optimal configuration (α, λ) such that the total heat current generated by the sector per unit of disc thickness,

$$q' = q''' \frac{\alpha}{2} R^2 \tag{5}$$

encounters minimal thermal resistance. The global temperature difference that drives the heat flow is $T_{\max} - T_{\min}$, where $T_{\max}$ is the hot spot temperature, and $T_{\min}$ is the temperature of the root of the fin. The rest of the disc perimeter is insulated. When the sector is very slender, the likely location of the hot spot is in the center of the disc, T_c. When the sector is not sufficiently slender, the hot spot may occur on the perimeter at the midpoint between two adjacent fin roots, T_h. In the following analysis we investigate both possibilities,

$$T_{\max} = \max(T_c, T_h) \tag{6}$$

The global thermal resistance to be minimized is

$$R_{\text{th}} = \frac{T_{\max} - T_{\min}}{q'} \tag{7}$$

A relatively simple analytical solution is possible based on the geometrical observation that the tip of the fin receives the heat current generated by the wedge of length $R - L$ and angle α,

$$q'_{\text{tip}} = q''' \frac{\alpha}{2} (R - L)^2 \tag{8}$$

As shown in the lower part of Fig. 2, the fin receives at every longitudinal position x the heat current collected in the $x =$ constant plane in the k_0 material, namely $q'' \, \mathrm{d}x$, where

$$q'' = q'''[\alpha(R - L + x) - D] \tag{9}$$

Conduction along the fin is described by

$$\frac{\mathrm{d}}{\mathrm{d}x}\left(- k_p D \frac{\mathrm{d}T}{\mathrm{d}x} \right) = q'' \tag{10}$$

Eliminating q'' between Eqs. (9) and (10), integrating twice, and invoking the boundary conditions

$$-k_p D \frac{\mathrm{d}T}{\mathrm{d}x}\bigg|_{x=0} = q'_{\text{tip}} \tag{11}$$

$$T = T_{\min} \quad \text{at} \quad x = L \tag{12}$$

we obtain the temperature distribution along the fin, $T(x)$. Finally, by writing $T_0 = T(0)$, we find the end-to-end temperature difference

$$T_0 - T_{\min} = \frac{q'''}{k_p D}\left[\frac{\alpha}{2}(R - L)LR + \frac{\alpha}{6} L^3 - \frac{D}{2} L^2 \right] \tag{13}$$

Next is the calculation of the temperature drop from the center (T_c) to the fin tip (T_0). Conduction in the wedge of length $(R - L)$ and material k_0 is described by

$$q'_* = -k_0 \alpha \xi \frac{\mathrm{d}T}{\mathrm{d}\xi} \tag{14}$$

$$\frac{\mathrm{d}q'_*}{\mathrm{d}\xi} = \alpha \xi q''' \tag{15}$$

Eliminating q'_* between Eqs. (14) and (15), integrating twice, and invoking the boundary conditions $T = T_c$ at $\xi = 0$, and $T = T_0$ at $\xi = R - L$, we find the temperature difference

$$T_c - T_0 = \frac{q'''}{4k_0}(R-L)^2 \tag{16}$$

The overall temperature difference between the disc center and the fin root $(T_c - T_{min})$ is the sum of Eqs. (13) and (16). With this and Eq. (7) we construct the dimensionless global thermal resistance

$$\widetilde{R}_c = \frac{T_c - T_{min}}{q'/k_0} \tag{17}$$

which assumes the form

$$\widetilde{R}_c = \frac{\lambda}{\tilde{k}}\left[1 - \frac{L}{R} + \frac{1}{3}\left(\frac{L}{R}\right)^2\right] + \frac{1}{2\alpha}\left[1 - 2\frac{L}{R} + \left(1 - \frac{2}{\tilde{k}}\right)\left(\frac{L}{R}\right)^2\right] \tag{18}$$

The ratio L/R is given by the ϕ constraint Eq. (1), which after using Eqs. (2) and (3) yields

$$\frac{L}{R} = \left(\frac{\alpha}{2}\phi\lambda\right)^{1/2} \tag{19}$$

The global conductance $\widetilde{R}_c$ emerges as a function of the two degrees of freedom of the configuration or $(\alpha, L/R)$, and the specified construction parameters $(\phi, \tilde{k})$, where

$$\tilde{k} = \frac{k_p}{k_0} \gg 1 \tag{20}$$

The preceding analysis is valid when Eq. (4) hold, and when the fin is thin enough so that it fits completely inside the slender sector. This last condition requires

$$D < \alpha(R-L) \tag{21}$$

which in view of Eq. (19) means

$$\left(1 + \frac{1}{\alpha\lambda}\right)\left(\frac{\alpha}{2}\phi\lambda\right)^{1/2} < 1 \tag{22}$$

Finally, we must account for the possibility that the hot spot is not in the center (T_c), but on the rim (T_h). The temperature difference $(T_h - T_{min})$ must be compared with $(T_c - T_{min})$, and the larger of the two must be minimized. The larger of the two is the global temperature difference $T_{max} - T_{min}$ that appears in the R_{th} definition, Eq. (7). Consider the generation of heat (q''') on the rim, on the short arc of length $(\alpha/2)R$ the ends of which are at temperatures T_h and T_{min}, Fig. 2. The points on this arc generate the heat current

$$q'' = q'''\frac{\alpha}{2}R \tag{23}$$

which arrives at the T_{min} root of the fin,

$$q'' = k_0\left.\frac{dT}{dy}\right|_{y=0} \tag{24}$$

The y coordinate is measured from $y = 0$ where $T = T_{min}$. Because of the uniformly distributed heat generation rate q''', the temperature distribution is parabolic versus y, with zero slope at $y = (\alpha/2)R$, where $T = T_h$. One can show that the slope at $y = 0$ is

$$\left.\frac{dT}{dy}\right|_{y=0} = 2\frac{T_h - T_{min}}{(\alpha/2)R} \tag{25}$$

By combining Eqs. (23)–(25), we find the largest temperature excursion on the rim,

$$T_h - T_{min} = q'''\frac{\alpha^2 R^2}{8k_0} \tag{26}$$

and the corresponding dimensionless thermal resistance defined as in Eq. (17),

$$\widetilde{R}_h = \frac{T_h - T_{min}}{q'/k_0} = \frac{\alpha}{4} \tag{27}$$

In summary, the objective is to minimize the larger of the thermal resistances derived in Eqs. (18) and (27),

$$\widetilde{R} = \max(\widetilde{R}_c, \widetilde{R}_h) \tag{28}$$

by varying α and λ, subject to condition Eq. (22) and fixed ϕ and $\tilde{k}$. Analytically, it is more convenient to start with Eqs. (18) and (19), express $\widetilde{R}_c$ as a function of α and L/R as free variables, and solve $\partial\widetilde{R}_c/\partial(L/R) = 0$ to determine the optimal fin length ratio L/R. The result is given implicitly by

$$\frac{2}{\phi\tilde{k}}\left(2\tilde{y} - 3\tilde{y}^2 + \frac{4}{3}\tilde{y}^3\right) + \left(1 - \frac{2}{\tilde{k}}\right)\tilde{y} = 1 \tag{29}$$

where $\tilde{y} = (L/R)_{opt}$. The optimal fin length is independent of α, but depends on $\tilde{k}$ and ϕ. While trying several plots of $(L/R)_{opt}$ versus $\tilde{k}$ for several values of ϕ, we found that the curves fall almost on top of each other if we use the group $\tilde{k}\phi$ on the abscissa. As shown in Fig. 3, the product $\tilde{k}\phi$ captures most of the effect of $\tilde{k}$ and ϕ on

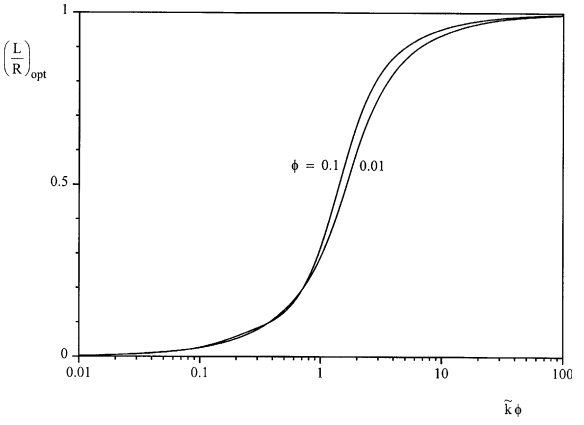

Fig. 3. The optimal fin length determined in Eq. (29).

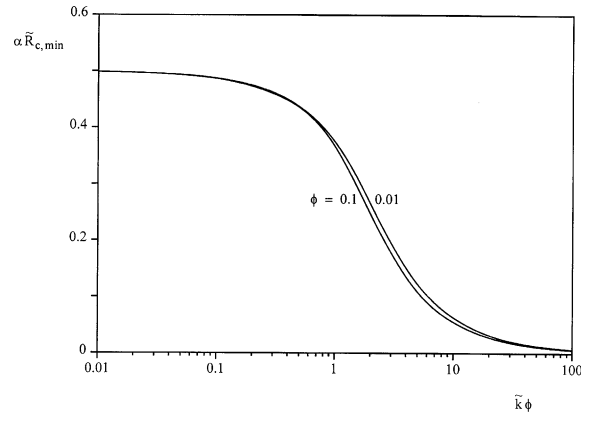

Fig. 4. The minimized global thermal resistance corresponding to the optimal fin length reported in Fig. 3.

$(L/R)_{opt}$. The *S*-shaped bundle of curves shows a transition when $\tilde{k}\ \phi$ is in the range 1–10. When $\tilde{k}\phi$ is smaller than 1, we see that $(L/R)_{opt} \to 0$, and the fins disappear. When $\tilde{k}\phi$ is greater than 10, the behavior is $(L/R)_{opt} \to 1$, and the fin tips almost touch in the center of the disc.

The minimized $\widetilde{R}_c$ function that corresponds to Eq. (29) and Fig. 3 is proportional to $1/\alpha$. This is why it is reported in Fig. 4 as $\alpha\widetilde{R}_{c,min}$ versus $\tilde{k}$ and ϕ. Again, we found that the curves almost collapse on a single curve if we use the product $\tilde{k}\phi$ on the abscissa. The transition is again marked by the range $1 < \tilde{k}\phi < 10$. The highest resistance ($\alpha\widetilde{R}_{c,min} = 0.5$) is when $\tilde{k}\phi < 1$, and the fins disappear. The lowest resistance ($\alpha R_{c,min} = 0$) is approached in the limit where $\tilde{k}\phi$ much greater than 10.

When we plotted $\alpha\widetilde{R}_{c,min}$ versus $\tilde{k}$ alone (for fixed values of ϕ), we found that diminishing returns are registered as the volume fraction of the radial fins ϕ increases. This means that when $\tilde{k}$ is fixed, the reduction in $\alpha\widetilde{R}_{c,min}$ is greater when ϕ increases from 0.01 to 0.05, than when ϕ increases from 0.05 to 0.1.

At this point it is important to recall Eqs. (27) and (28) in order to understand the emphasis placed on the $\alpha\widetilde{R}_{c,min}$ group in the preceding discussion. From Fig. 4 it is clear that the highest thermal resistance between the center of the disc and the fin root is $\alpha\widetilde{R}_{c,min} = 0.5$. According to Eq. (27), such a dimensionless thermal resistance is reached when $\alpha\widetilde{R}_{h,min} = 0.5$ or $\alpha = 2^{1/2}$, which would violate the first of Eq. (4). This means that in the domain where analysis is valid, the hot spot temperature always occurs in the center of the disc.

3. Numerical formulation

The objective of this second phase of the work was to calculate and minimize numerically the hot spot temperature on the sector shown in Fig. 2. Two degrees of freedom were considered: the number of sectors, which is represented by the angle α, and the aspect ratio of the fin $\lambda = L/D$.

The numerical domain was divided in two regions: the disc material with low conductivity material k_0 and volumetric heat generation q''', and the high-conductivity plate fin. The conduction in the disc domain is ruled by

$$k_0 \nabla^2 T = -q''' \tag{30}$$

For the fin domain, the energy equation reads

$$k_p \nabla^2 T = 0 \tag{31}$$

Because of symmetry, all the boundaries of the sector were modeled as adiabatic $\partial T/\partial n = 0$, where n is the vector normal to the respective boundary. Two different thermal boundary conditions were imposed on the fin: constant temperature at the fin root T_{min}, and flux continuity at the interface between the k_p fin and the k_0 disc. Neglecting the thermal contact resistance between the disc and the fin, the heat flux continuity in the interface is

$$k_0 \left.\frac{\partial T}{\partial n}\right|_{disc} = k_p \left.\frac{\partial T}{\partial n}\right|_{fin} \tag{32}$$

The nondimensionalization of Eqs. (30)–(32) was made using the dimensionless variables

$$(\tilde{x}, \tilde{y}, \widetilde{L}, \widetilde{D}) = \frac{(x, y, L, D)}{R}, \quad \widetilde{T} = \frac{T - T_{min}}{q''' R^2/k_0} \tag{33}$$

The steady-state heat conduction problem defined in Fig. 2 was solved using an available finite elements code [15]. Triangular elements were used. The grid was refined in the vicinity of the wedges of the disc, where high temperature gradients are expected. Grid accuracy tests were performed for all configurations reported in this section. The convergence criterion was based on the comparison of the $\widetilde{T}_{max}$ results of a less refined mesh (mesh 1), and a more refined mesh (mesh 2), until the following convergence criterion was satisfied

$$\varepsilon = \left\| \frac{\widetilde{T}_{max}(\text{mesh 1}) - \widetilde{T}_{max}(\text{mesh 2})}{\widetilde{T}_{max}(\text{mesh 2})} \right\| \leqslant 0.001 \tag{34}$$

Fig. 5 shows the variation of the maximum temperature on the disc versus the aspect ratio of the fin for fixed values of ϕ and N (or α). An immediate conclusion is that the optimization of the fin aspect ratio is useful because the curves for $\tilde{k} > 10$ are not flat. Minimum values of $\widetilde{T}_{max}$ are obtained for fins with high aspect ratios, i.e., $\lambda \gg 1$. Another important feature presented in Fig. 5 is the effect of the conductivity ratio on $\widetilde{T}_{max}$: diminishing returns are reached as $\tilde{k}$ increases.

Fig. 6 shows the effect of the fin volume fraction ϕ on $\widetilde{T}_{max}$. The disc thermal resistance decreases as the

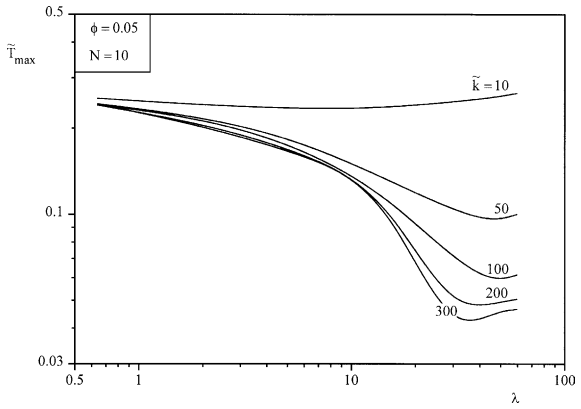

Fig. 5. Numerical minimization of the global thermal resistance with respect to the fin aspect ratio: the effect of $k = k_p/k_0$.

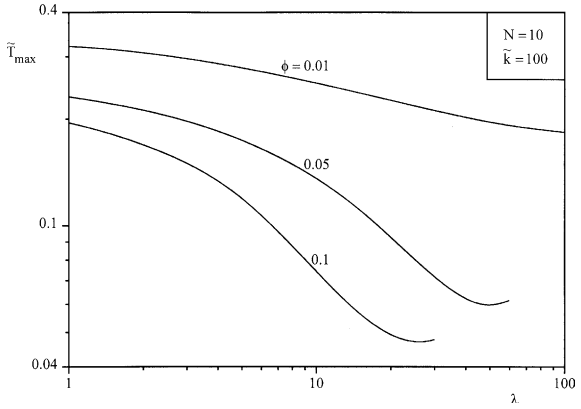

Fig. 6. Numerical minimization of the global thermal resistance with respect to the fin aspect ratio: the effect of ϕ.

slenderness and the area fraction of the fin increase. Diminishing returns are also evident as ϕ increases.

Fig. 7 shows that the optimal fin aspect ratio λ_{opt} increases with the number of sectors for the three values

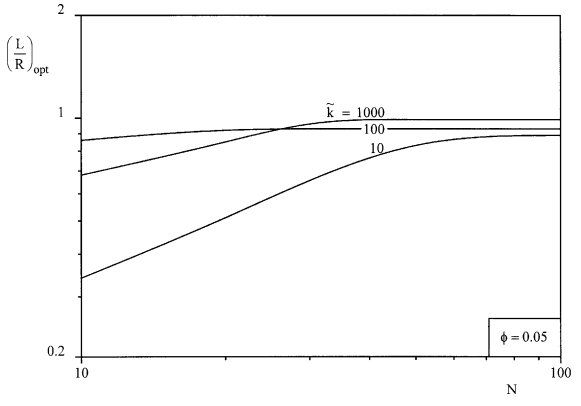

Fig. 7. The optimal fin length determined numerically.

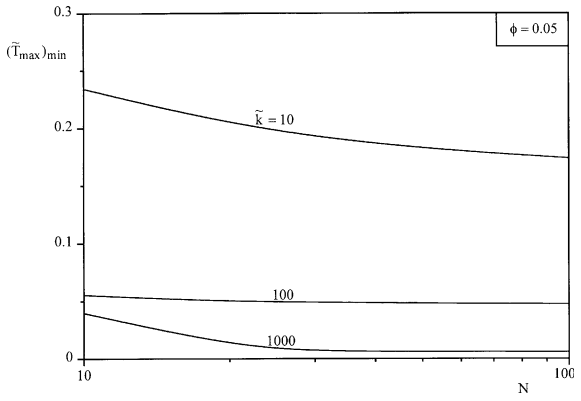

Fig. 8. The minimized global thermal resistance determined numerically.

of $\tilde{k}$ considered. It is worth mentioning that for $N \geqslant 50$ the optimal fin length was practically constant, and depends only on $\tilde{k}$. This means that the behavior presented in Fig. 7 is mainly due to the reduction in the fin thickness $\widetilde{D}_{opt}$ as the number of sectors increases. This trend was predicted analytically in Eq. (29).

Fig. 8 shows that the minimized global resistance $(\widetilde{T}_{max})_{min}$ decreases as the number of optimized sectors increase. Although there is no optimal number of sectors, the $(\widetilde{T}_{max})_{min}$ curves become horizontal at large values of N. In this limit, the minimized global conductance is independent of the number of sectors on the disc.

4. Conclusions

In this paper we showed analytically and numerically that the geometry of rectangular high-conductivity inserts in a disc-shaped body that generates heat at every point can be optimized for minimal thermal resistance. In addition, we showed that the optimal design is highly dependent on the construction parameters N, ϕ and $\tilde{k}$. These developments reinforce the main line of the constructal method, which holds that the maximization of flow access (e.g., heat, fluid, etc.) subject to global constraints is the mechanism that generates the flow architecture.

An important question is whether the analytical solution agrees with the numerical results. Fig. 9 shows the comparison between the analytical solution of the optimal fin length, Eq. (29), and the numerical results when the disc has one hundred fins. In spite of the simplicity of our analytical model, the agreement is good in an order of magnitude sense, especially when $\tilde{k} \gg 100$, regardless of ϕ. In this limit $(L/R)_{opt}$ approaches 1. For low $\tilde{k}$ values, $\tilde{k} \ll 100$, the numerical results are insensitive to $\tilde{k}$ especially at sufficiently high $\phi \geqslant 0.05$.

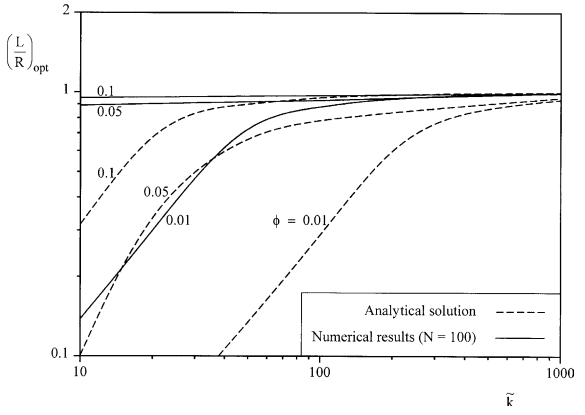

Fig. 9. Optimal fin lengths: comparison between the analytical solution and the numerical results.

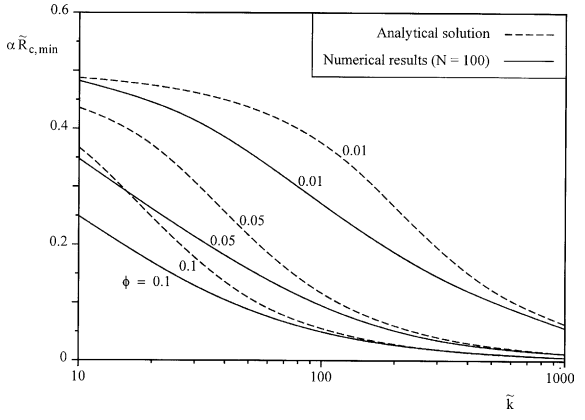

Fig. 10. Minimal thermal resistances: comparison between the analytical solution and the numerical results.

In the same limit, the analytical solution behaves differently. The reason is that the analytical solution is valid only when Eq. (4) holds. For $\phi = 0.01$, the numerical and analytical results exhibit similar trends.

Fig. 10 shows a comparison between the numerical results and the analytical solution for the minimal thermal resistance $\alpha\widetilde{R}_{c,min}$. The agreement is good in the range $10 < \tilde{k} < 1000$ and $0.01 < \phi < 0.1$. The two solutions agree much better as $\tilde{k}$ increases. This is consistent with assumptions Eq. (4), which indicate the range of validity of the analytical solution.

Acknowledgements

A.K. da Silva's work was fully supported by the Brazilian Research Council—CNPq under the doctoral scholarship No. 200021/01-0. The problem formulated in this paper resulted from group discussions held with Profs. M. Feidt and R. Boussehain at the University Henri Poincaré in Nancy, France, in February 2003. We also thank Profs. Feidt and Boussehain for their comments on this manuscript.

References

[1] A. Bejan, Shape and Structure, from Engineering to Nature, Cambridge University Press, Cambridge, UK, 2000.
[2] A. Bejan, I. Dincer, S. Lorente, A.F. Migueln, A.H. Reis, Porous and Complex Flow Structures in Modern Technologies, Springer-Verlag, New York, 2004.
[3] A. Bejan, S. Lorente, The constructal law and the thermodynamics of flow systems with configuration, Int. J. Heat Mass Transfer 47 (2004) 3203–3214.
[4] R.A. Meric, Boundary elements for joule heating of solids with orthotropic conductivities, Eng. Anal. Bound. Elem. 20 (1997) 253–260.
[5] G. Fabbri, A genetic algorithm for fin profile optimization, Int. J. Heat Mass Transfer 40 (1997) 2165–2172.
[6] R.A. Meric, Shape design sensitivity analysis and optimization for nonlinear heat and electric conduction problems, Num. Heat Transfer A 2 (1998) 185–203.
[7] G. Fabbri, Optimum profiles for asymmetrical longitudinal fills in cylindrical ducts, Int. J. Heat Mass Transfer 42 (1999) 511–523.
[8] C.H. Cheng, C.Y. Wu, An approach combining body-fitted grid generation and conjugate gradient methods for shape design in heat conduction problems, Num. Heat Transfer B 37 (2000) 69–83.
[9] C.H. Lan, C.H. Cheng, C.Y. Wu, Shape design for heat conduction problems using curvilinear grid generation, conjugate gradient, and redistribution methods, Numer. Heat Transfer A 39 (2001) 487–510.
[10] C.H. Cheng, H.H. Lin, W. Aung, Optimal shape design for packaging containing heating elements by inverse heat transfer method, Heat Mass Transfer 39 (2003) 687–692.
[11] M.Q. Zou, B.M.N. Yu, D.M. Zhang, Y.T. Ma, Study on optimization of transverse thermal conductivities of unidirectional composites, J. Heat Transfer 125 (2003) 980–987.
[12] A.D. Kraus, A. Aziz, J. Welty, Extended Surface Heat Transfer, Wiley, New York, 2001.
[13] L.A.O. Rocha, S. Lorente, A. Bejan, Constructal design of cooling disc-shaped area by conduction, Int. J. Heat Mass Transfer 45 (2002) 1643–1652.
[14] J. Bonjour, L.A.O. Rocha, A. Bejan, F. Meunier, Dendritic fins optimization for a coaxial two-stream heat exchanger, Int. Heat Mass Transfer 47 (2004) 111–124.
[15] MATLAB-Partial Differential Equation Toolbox, The MathWorks, Inc., Natick, MA, 2002.